ELSEVIER

PII: S0032-3861(98)00128-1

Polymer Vol. 39 No. 26, pp. 6905–6910, 1998

0032-3861/98/$ - see front matter

Phase behaviours of polymer solutions in high pressure system

In Ha Kim, Jeong Gyu Jang and Young Chan Bae*
Department of Industrial Chemistry and Molecular Thermodynamics Laboratory, Hanyang University, Seoul 133-791, South Korea
(Revised 3 February 1998)

A modified generalized lattice-fluid (MGLF) model was developed to predict and describe phase behaviours of polymer solutions under high pressure condition. To consider the specific interaction between pure components, a new parameter, κ_{11}, was introduced into the generalized lattice-fluid (GLF) model. The proposed model was compared with a phase diagram predicted by the GLF model and experimental data for polymer solution systems (polystyrene/diethylether and polystyrene/acetone) showing lower critical solution temperature (LCST) at various pressures. The MGLF model predicted remarkably well the spinodal curve of a given polymer/solvent system.

(Keywords: high-pressure; generalized lattice-fluid model; specific interaction)

INTRODUCTION

The factors we must consider during the manufacture of polymers are rheological properties, mechanical properties of polymer products, and sometimes, phase equilibria of polymer solutions in reactors necessarily. Since polymer synthesis reaction does not go to completion, polymer mixtures should be separated not only to gain polymer products but to recover unreacted monomers for recycle. In most cases, polymer production processes are executed at very high temperature and pressure. And due to the condition in the reactor, polymer/monomer mixtures consist of one phase or more. For example, polyethylene/ethylene mixture exists in one phase under about 3 000 atm and 300°C, however, after compression and cooling up to 900 atm and 260°C, the mixture is separated into two phases — polyethylene rich phase and ethylene rich phase. It is very desirable to develop a molecular thermodynamic framework in the prediction of phase behaviours of polymer/solvent systems for high temperature and pressure condition.

To understand the phase behaviours of polymer/solvent mixtures, various kinds of polymer solution theories have been developed. Flory and Huggins[1–3] proposed a closed-packed lattice model of which cells are all occupied by segments of molecules — solvents and polymers. However, this theory gives too narrow liquid–liquid coexistence curve when compared with experimental data and moreover, this model could not explain effect of pressure satisfactorily because of not considering compressibility. In advance, two other classes of models were developed, so-called lattice-fluid model and hole theories[4]. In these theories holes, or vacant cells, are introduced in the lattice to describe the extra entropy of change in the system caused by pressure and temperature.

The size of entire lattice is fixed and the appearance of new holes only causes volume changes. As a similar treatment, Kleintjens and Koningsveld[5,6] developed a mean-field lattice-gas (MFLG) equation of state to predict liquid–liquid phase separation of a polymer/solvent system. van Opstal and Koningsveld[7] investigated the effect of pressure on the polystyrene/cyclohexane system using this equation. Heil and Prausnitz[8], Brandini[9], Panayiotou and Vera[10] developed a polymer solution theory taken into account of a local composition. Bae *et al.*[11–13] reported the extended Flory–Huggins theory for binary polymer system. Sanchez and Lacombe[14,15] developed a lattice-fluid (LF) model accounting for compressibility and volume changes. A similar approach was followed by Arai and Saito[16]. Later, Panayiotou[17] and Sanchez and Balazs[18] generalized the LF model to account for the specific interaction.

The phase behaviours of mixtures under high pressure condition has had an attracted interest since the end of the past century. van der Waals[5] has pointed out the peculiarity of the behaviour of fluid mixtures at elevated pressure and predicted the possibility of phase separation. Prigogine *et al.*[19] tried a theoretical approach to the research on the effect of pressure using the components P-V-T data. Guggenheim[20] developed a two-component lattice model for the prediction of phase behaviour of low molecular weight mixtures. However, this model was not suitable for vapor–liquid equilibria because Guggenheim assumed the partial specific densities of each component to be the same in each phase. Trappaniers *et al.*[21] tried to solve this shortcoming by introducing the concept of lattice-gas model developed for one component by Mulholland *et al.*[22] Bonner *et al.*[23] calculated phase equilibria of the polyethylene/ethylene system at 260°C and at 200, 500 and 900 atm using the statistical mechanical theory developed by Prigogine and Flory. In the similar treatment, Zeman *et al.*[24] investigated the effect of pressure on the phase equilibria of polymer solutions in the temperature range of 0–200°C for polyisobutylene with various molecular weights in short-chain alkanes (C_3–C_6) and of polydimethylsiloxane in C_2–C_4. He found that pressure displaces the phase boundary associated with the LCST to higher temperatures, i.e., increases polymer solubility. Liu and Prausnitz[25] applied

* To whom correspondence should be addressed

the perturbed-hard-chain theory (PHCT) including two binary parameters to phase equilibrium calculation for mixtures of ethylene and low-density polyethylene from ambient pressure to 2000 atm. Sako *et al.*[26] used generalized van der Waals partition function to obtain a new three-parameter cubic equation of state which is applicable to fluids containing small or large molecules, including polymers. Upon extension to mixtures, the equation of state was able to be used for calculation of high-pressure phase equilibria for the ethylene/polyethylene system. In this study, we tried a new approach to the understanding of the pressure effect on the polymer solution thermodynamic property in high pressure system. Jang *et al.*[27] modified GLF theory at zero pressure to account for the specific interaction by introducing a new parameter. Based on this treatment, an extension of this model to the polymer/solvent system under high pressure was executed. The results of comparison are followed by this section.

MODEL DEVELOPMENT

In this study, all the expressions for thermodynamic model framework are about binary mixture of N_1 molecules of size r_1 and N_2 molecules of size r_2 (an r-mer occupies r sites on lattice of coordination number z).

The free energy of mixing

In the lattice-fluid (LF) model, free energy of mixing G is given by[14]

$$\frac{G}{rN\varepsilon^*} = -\tilde{\rho} + \tilde{p}\tilde{v} - \frac{\tilde{T}}{k}(S_{\text{comb}} + S_{\text{vac}}) \tag{1}$$

In this lattice, $rN = (r_1N_1 + r_2N_2)$ is defined as total lattice sites occupied by all segments of molecules in lattice. S_{comb} is a well-known combinatorial entropy of mixing and S_{vac} is an entropy of mixing holes in lattice with molecules given by

$$-\frac{S_{\text{comb}}}{k} = \frac{\phi_1}{r_1}\ln\phi_1 + \frac{\phi_2}{r_2}\ln\phi_2 \tag{2}$$

$$-\frac{S_{\text{vac}}}{k} = \frac{1-\tilde{\rho}}{\tilde{\rho}}\ln(1-\tilde{\rho}) + \frac{\ln\tilde{\rho}}{r} \tag{3}$$

We set free energy per a molecule G/rN is f, then equation (1) yields

$$f = -\tilde{\rho}\varepsilon^* + \frac{Pv^*}{\tilde{\rho}} - T(S_{\text{comb}} + S_{\text{vac}}) \tag{4}$$

where ε* is the mixing interaction energy.

In case of a binary system of LF model, N_1r_1-mers, N_2r_2-mers and N_0 vacancies should be packed on lattice sites of $N_0 + r_1N_1 + r_2N_2$. The number of ways of distributing molecules on the lattice Ω is obtained by inserting one molecule at a time onto the lattice. In this way, Ω can be expressed as

$$\Omega = \Omega_{\text{ends}}\Omega_{r-1} \tag{5}$$

where Ω_{ends} is the number of ways of distributing $N_1 + N_2$ polymer chain ends on the lattice of rN sites. Under the rough assumption that both r_1 and r_2 are large enough, Ω_{ends} can be simply expressed using Stirling's approximation as

$$\Omega_{\text{ends}} = \left(\frac{r_1 e}{\phi_1}\right)^{N_1}\left(\frac{r_2 e}{\phi_2}\right)^{N_2} \tag{6}$$

Ω_{r-1} is the number of ways that the remaining $r_1 - 1$ mers of each molecule 1 and $r_2 - 1$ mers of each molecule 2 can be arranged:

$$\Omega_{r-1} = \left(\frac{\delta_1}{e^{r_1}}\right)^{N_1}\left(\frac{\delta_2}{e^{r_2}}\right)^{N_2} \tag{7}$$

where δ_i is the polymer flexibility parameter.

Combining equation (6) with equation (7) yields the well-known Flory results,

$$\Omega = \left(\frac{\omega_1}{\phi_1}\right)^{N_1}\left(\frac{\omega_2}{\phi_2}\right)^{N_2} \tag{8}$$

where $\omega_i = r_i\delta_i/e^{r_i-1}$.

Some parameter values for the LF equation of state are listed in *Table 1*. As seen in *Table 1*, size parameters of the most solvents are smaller than 15. It causes a serious error because the Stirling's approximation can be applied only to large value of r. For this reason, the GLF model shows a large deviation from experimental data when applied to polymer/solvent systems. Jang *et al.*[27] introduced a new universal parameter C_0 to solve this problem as below

$$\bar{r}_1 = C_0 r_1, \quad \frac{1}{\bar{r}} = \frac{\phi_1}{\bar{r}_1} + \frac{\phi_2}{r_2} \tag{9}$$

As shown in *Figure 1*, the spinodal curve converses to the expected critical point region and finally coincides with the experimental data when $C_0 = 100$. These results hold irrespective of C_0 as far as its value is much larger than 100. As a result, they proposed that the optimum value for C_0 is 100. It is not an adjustable parameter but a universal constant. In addition, they introduced a parameter κ_{11} to consider the effect of specific interaction among pure components neglected by Sanchez *et al*. The new expressions for the free energy of mixing denoted by f_E and interaction energy ϵ* can be written as

$$f_E = -\tilde{\rho}\varepsilon^* + \frac{Pv^*}{\tilde{\rho}} - T(S_{\text{comb}} + S_{\text{vac}}) \tag{10}$$

$$\varepsilon^*(\phi, T) = \phi_1^2\varepsilon_{11}^*(1-\kappa_{11}) + 2\phi_1\phi_2 f_{12}^* + \phi_2^2\varepsilon_{22}^* \tag{11}$$

$$-\frac{S_{\text{comb}}}{k} = \frac{\phi_1}{\bar{r}_1}\ln\phi_1 + \frac{\phi_2}{r_2}\ln\phi_2 \tag{12}$$

$$-\frac{S_{\text{vac}}}{k} = \frac{1-\tilde{\rho}}{\tilde{\rho}}\ln(1-\tilde{\rho}) + \frac{\ln\tilde{\rho}}{\bar{r}} \tag{13}$$

This model reduces to GLF model when $\kappa_{11} = 0$ and both r_1 and r_2 are large enough ($C_0 = 1$).

The equation of state

The free energy of mixing is a minimum when

$$\frac{\partial G}{\partial \tilde{v}}\Big|_{T,P,\phi} = 0 \text{ or equivalently } \frac{\partial f_E}{\partial \tilde{\rho}}\Big|_{T,P,\phi} = 0 \tag{14}$$

Table 1 List of characteristic parameters for Lattice Fluid Equation of State

Fluid	T* (K)	P* (MPa)	ρ* (kg m^{-3})	r
Methane	224	248	500	4.26
Pentane	441	310	755	8.09
Diethylether	431	363	870	8.62
Cyclohexane	497	383	902	8.65
Acetone	484	533	917	8.40
Ethyl acetate	468	458	1052	9.87

which yields the lattice fluid equation of state

$$\tilde{\rho}^2+\tilde{P}+\tilde{T}\left(\ln(1-\tilde{\rho})+\left(1-\frac{1}{\bar{r}}\right)\tilde{\rho}\right)=0 \qquad (15)$$

and this can be rewritten:

$$(\tilde{\rho}^2\varepsilon^*+Pv^*)\beta+\ln(1-\tilde{\rho})+\left(1-\frac{1}{\bar{r}}\right)\tilde{\rho}=0 \qquad (16)$$

where $\beta = 1/kT$ and $v^* = \sum_i \phi_i v_i^* = \phi_1 v_1^* + \phi_2 v_2^*$.

The chemical potentials and critical conditions

The chemical potential for component 1 in a binary mixture is given by

$$\mu_1 = \bar{r}_1\left(f_E+\phi_2\frac{df_E}{d\phi_1}\right) \qquad (17)$$

The free energy of mixing f_E is a function of ϕ, $\tilde{\rho}$, ε*, v* and $\bar{r}$, and simultaneously $\tilde{\rho}$, ε*, v* and $\bar{r}$ are all the function of ϕ. Using chain rule, $df_E/d\phi_1$ can be obtained by

$$\frac{df_E}{d\phi_1}=\frac{\partial f_E}{\partial\phi_1}+\frac{\partial f_E}{\partial\tilde{\rho}}\frac{\partial\tilde{\rho}}{\partial\phi_1}+\frac{\partial f_E}{\partial\varepsilon^*}\frac{\partial\varepsilon^*}{\partial\phi_1}+\frac{\partial f_E}{\partial v^*}\frac{\partial v^*}{\partial\phi_1}+\frac{\partial f_E}{\partial\bar{r}}\frac{\partial\bar{r}}{\partial\phi_1} \qquad (18)$$

and from the equation of state, $\frac{\partial\tilde{\rho}}{\partial\phi_1}$ can be obtained as below

$$\left[2\tilde{\rho}\varepsilon^*\frac{\partial\tilde{\rho}}{\partial\phi_1}+\tilde{\rho}^2\frac{\partial\varepsilon^*}{\partial\phi_1}+P(v_1^*-v_2^*)\right]\beta-\frac{1}{1-\tilde{\rho}}\frac{\partial\tilde{\rho}}{\partial\phi_1} -\left(\frac{1}{\bar{r}_1}-\frac{1}{r_2}\right)\tilde{\rho}+\left(1-\frac{1}{\bar{r}}\right)\frac{\partial\tilde{\rho}}{\partial\phi_1}=0 \qquad (19)$$

$$\frac{\partial\tilde{\rho}}{\partial\phi_1}=\frac{-\tilde{\rho}^2\beta\dfrac{\partial\varepsilon^*}{\partial\phi_1}-P\beta(v_1^*-v_2^*)+\tilde{\rho}\left(\dfrac{1}{\bar{r}_1}-\dfrac{1}{r_2}\right)}{2\tilde{\rho}\beta\varepsilon^*-\dfrac{1}{1-\tilde{\rho}}+\left(1-\dfrac{1}{\bar{r}}\right)} \qquad (20)$$

then the expression for μ_1 is

$$\frac{\mu_1}{\bar{r}_1}=-\tilde{\rho}\varepsilon^*+\frac{Pv_1^*}{\tilde{\rho}}-\tilde{\rho}\phi_2\frac{\partial\varepsilon^*}{\partial\phi_1} +kT\left(\frac{1}{\bar{r}_1}(\ln\phi_1+\phi_2)-\frac{\phi_2}{r_2}+\frac{\ln\tilde{\rho}}{\bar{r}_1}+\frac{1-\tilde{\rho}}{\tilde{\rho}}\ln(1-\tilde{\rho})\right) \qquad (21)$$

Similarly, the expression for μ_2 is

$$\frac{\mu_2}{\bar{r}_2}=-\tilde{\rho}\varepsilon^*+\frac{Pv_2^*}{\tilde{\rho}}-\tilde{\rho}\phi_1\frac{\partial\varepsilon^*}{\partial\phi_2} +kT\left(\frac{1}{r_2}(\ln\phi_2+\phi_1)-\frac{\phi_1}{\bar{r}_1}+\frac{\ln\tilde{\rho}}{r_2}+\frac{1-\tilde{\rho}}{\tilde{\rho}}\ln(1-\tilde{\rho})\right) \qquad (22)$$

The critical condition is given by

$$\frac{d\mu}{d\phi_1}=\frac{d^2\mu}{d\phi_1^2}=0,\ \text{or equivalently}\ \frac{d^2f_E}{d\phi_1^2}=\frac{d^3f_E}{d\phi_1^3}=0 \qquad (23)$$

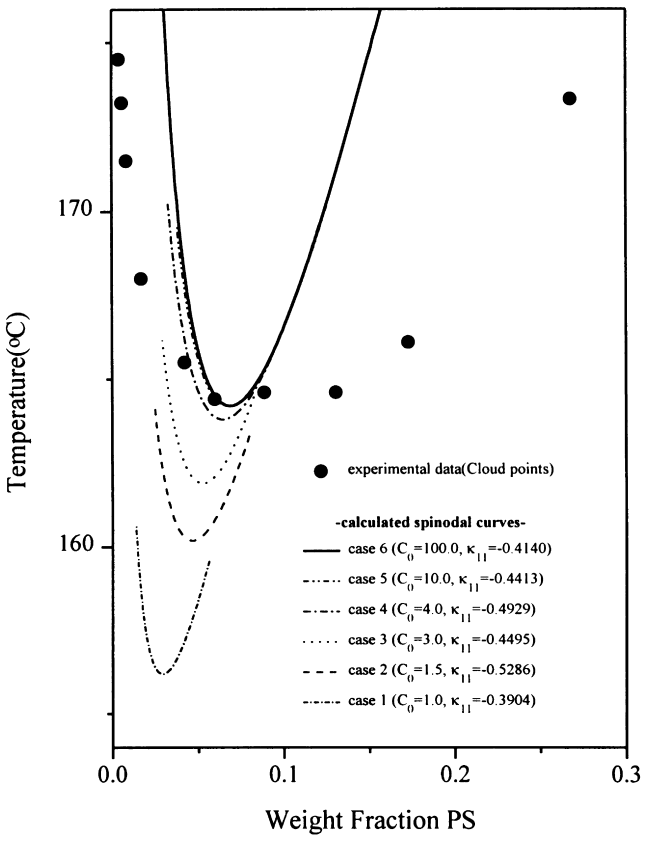

Figure 1 Cloud-point data for PS(Mw = 100 000;Mw/Mn < 1.06)/ethylacetate system. The solid line is calculated by this proposed model. The solid circles are experimental data by Bae *et al.*[28]

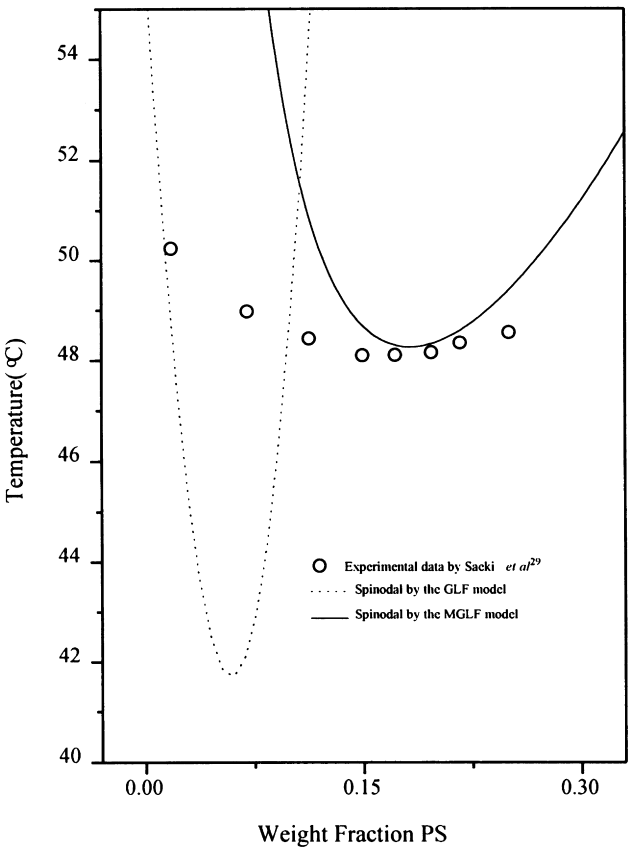

Figure 2 Cloud-point data for PS(Mw = 20 400;Mw/Mn < 1.05)/diethylether system at 10 atm. The dotted and the solid line are spinodal curves calculated by the GLF model and the MGLF model, respectively. Energy parameter values for the GLF model are $\varepsilon_{12}^*/k = 598.99$ K and $\delta\varepsilon^*/k = 683.65$ K. Values of adjustable model parameters for the MGLF model are $\varepsilon_{12}^*/k = 522.19$ K, $\delta\varepsilon^*/k = 1174.53$ K, and $\kappa_{11} = -0.4215$. The open circles are experimental data by Saeki *et al.*[29]

By setting $df_E/d\phi_1 = f_E'$, $d^2f_E/d\phi_1^2$ can be calculated as below

$$\frac{d^2f_E}{d\phi_1^2} = \frac{df_E'}{d\phi_1} = \frac{\partial f_E'}{\partial \phi_1} + \frac{\partial f_E'}{\partial \tilde{\rho}}\frac{\partial \tilde{\rho}}{\partial \phi_1} + \frac{\partial f_E'}{\partial \varepsilon^*}\frac{\partial \varepsilon^*}{\partial \phi_1} + \frac{\partial f_E'}{\partial v^*}\frac{\partial v*}{\partial \phi_1} + \frac{\partial f_E'}{\partial \bar{r}}\frac{\partial \bar{r}}{\partial \phi_1} \quad (24)$$

Differentiating equation (2) yields $\frac{\partial^2 \tilde{\rho}}{\partial \phi_1^2}$

$$\frac{\partial^2 \tilde{\rho}}{\partial \phi_1^2} = -\frac{\tilde{\rho}^2\beta\frac{\partial^2 \varepsilon^*}{\partial \phi_1^2} + \frac{\partial \tilde{\rho}}{\partial \phi_1}\left(4\tilde{\rho}\beta\frac{\partial \varepsilon^*}{\partial \phi_1} + \left(2\beta\varepsilon^* - \frac{1}{(1-\tilde{\rho})^2}\right)\frac{\partial \tilde{\rho}}{\partial \phi_1} - 2\left(\frac{1}{\bar{r}_1} - \frac{1}{r_2}\right)\right)}{2\tilde{\rho}\beta\varepsilon^* - \frac{1}{1-\tilde{\rho}} + \left(1 - \frac{1}{\bar{r}}\right)} \quad (25)$$

In the same way, $d^3f_E/d\phi_1^3$ can be calculated by setting $d^2f_E/d\phi_1^2 = f_E''$

$$\frac{d^3f_E}{d\phi_1^3} = \frac{df_E''}{d\phi_1} = \frac{\partial f_E''}{\partial \phi_1} + \frac{\partial f_E''}{\partial \tilde{\rho}}\frac{\partial \tilde{\rho}}{\partial \phi_1} + \frac{\partial f_E''}{\partial \varepsilon^*}\frac{\partial \varepsilon^*}{\partial \phi_1} + \frac{\partial f_E''}{\partial v^*}\frac{\partial v^*}{\partial \phi_1} + \frac{\partial f_E''}{\partial \bar{r}}\frac{\partial \bar{r}}{\partial \phi_1} \quad (26)$$

RESULTS AND DISCUSSIONS

The proposed MGLF model has three adjustable model parameters, ε_{12}, $\delta\varepsilon$, and κ_{11} and a universal constant, C_0. A parameter, κ_{11}, is introduced only to 1–1 interaction because ε_{11}^* is much more sensitive in the calculation of spinodal curve than that of ε_{22}^*.

Figure 1 represents a phase diagram of PS(Mw = 100 000;Mw/Mn < 1.06)/ethylacetate system. Solid circles are experimental cloud point data by Bae *et al.*[28]. As shown in *Figure 1*, the critical point converses to the experimental critical point as C_0 is closer to 100. In this study, we fixed at $C_0 = 100$.

Figure 2 shows cloud point data for PS(Mw = 20 400; Mw/Mn < 1.05)/diethylether system which shows a LCST behaviour reported by Saeki *et al.*[29]. The measured pressure was 10 atm. The solid line is calculated by the MGLF model with $C_0 = 100$. The dotted line is calculated in the case of $C_0 = 1$ that is the GLF model. There is a slight deviation between a critical point predicted by the MGLF model and a measured critical point. The GLF model ($C_0 = 1$) shows a large deviation from the expected value. Energy parameter values for the GLF model are $\varepsilon_{12}^*/k = 598.99$ K and $\delta\varepsilon^*/k = 683.65$ K. Values of adjustable model parameters for the MGLF model are $\varepsilon_{12}^*/k = 522.19$ K, $\delta\varepsilon^*/k = 1174.53$ K, and $\kappa_{11} = 0.4215$. It means that the GLF model underestimated ε_{11}^* by about 42%.

Figure 3 shows a phase diagram of PS(Mw = 20 400;Mw/Mn < 1.05)/diethylether system at 20 atm reported by Saeki *et al.*[29]. The dotted line and the solid line are calculated spinodal curves by the GLF model and the MGLF model, respectively. Energy parameter values for

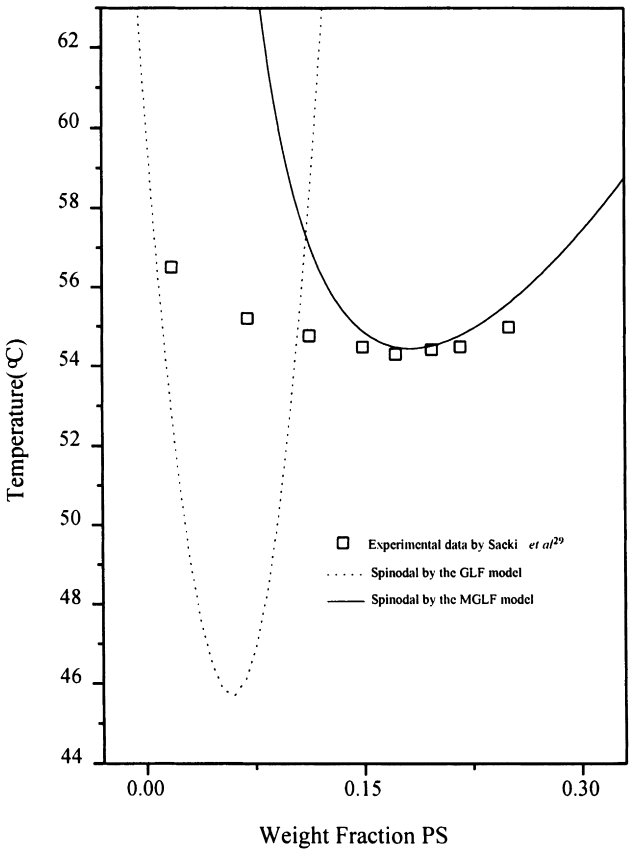

Figure 3 Cloud-point data for PS(Mw = 20 400;Mw/Mn < 1.05)/diethylether system at 20 atm. The dotted and the solid line are spinodal curves calculated by the GLF model and the MGLF model, respectively. Energy parameter values for the GLF model are $\varepsilon_{12}^*/k = 592.11$ K and $\delta\varepsilon^*/k = 696.38$ K. Values of adjustable model parameters for the MGLF model are $\varepsilon_{12}^*/k = 518.18$ K, $\delta\varepsilon^*/k = 1203.29$ K, and $\kappa_{11} = -0.4210$. The open squares are experimental data by Saeki *et al.*[29]

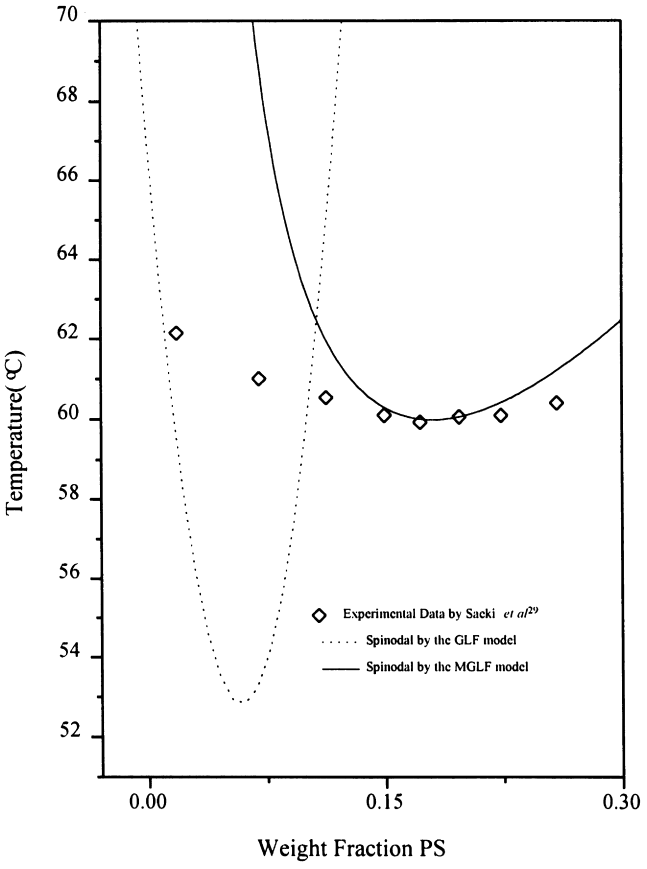

Figure 4 Cloud-point data for PS(Mw = 20 400;Mw/Mn < 1.05)/diethylether system at 30 atm. The dotted and the solid line are spinodal curves calculated by the GLF model and the MGLF model, respectively. Energy parameter values for the GLF model are $\varepsilon_{12}^*/k = 581.85$ K and $\delta\varepsilon^*/k = 776.25$ K. The adjustable model parameters for the MGLF model are $\varepsilon_{12}^*/k = 493.64$ K, $\delta\varepsilon^*/k = 1331.12$ K, and $\kappa_{11} = -0.3918$. The open diamonds are experimental data by Saeki *et al.*[29]

the GLF model are $\varepsilon^*_{12}/k = 592.11$ K and $\delta\varepsilon^*/k = 696.38$ K. Model parameter values for the MGLF model are $\varepsilon^*_{12}/k = 518.18$ K, $\delta\varepsilon^*/k = 1203.29$ K, and $\kappa_{11} = -0.4210$. From the value of κ_{11}, we can infer that the GLF model underestimated ε^*_{11} by about 42%. In this system, a critical point calculated by the MGLF model agrees very well with that of experimental data. The GLF model also predicts the critical point much lower than that of the experimental value.

Figure 4 shows a phase diagram of PS(Mw = 20 400;Mw/Mn < 1.05)/diethylether system under the condition of 30 atm reported by Saeki *et al.*[29]. Again, the dotted line and the solid line are calculated spinodal curves by the GLF model and the MGLF model, respectively. Energy parameter values for the GLF model are $\varepsilon^*_{12}/k = 581.85$ K and $\delta\varepsilon^*/k = 776.25$ K. Values of adjustable model parameters for the MGLF model are $\varepsilon^*_{12}/k = 493.64$ K, $\delta\varepsilon^*/k = 1331.12$ K, and $\kappa_{11} = -0.3918$. In this system, ε^*_{11} is also underestimated about 39% in the GLF model. The MGLF model predicts very well the critical point of a given system, however the GLF model shows a serious deviation from the experimental value. In PS/diethylether systems, values of ε^*_{12}/k decreases with increasing pressure, while $\delta\varepsilon^*/k$ increases with pressure.

Figure 5 shows a phase diagram of PS(Mw = 20 400;Mw/Mn ≅ 1.06)/acetone system at 20 bar reported by Zeman *et al.*[24]. The dotted line and the solid line are calculated spinodal curves by the GLF model and the MGLF model, respectively. Energy parameter values for the GLF model are $\varepsilon^*_{12}/k = 589.40$ K and $\delta\varepsilon^*/k = 690.21$ K.

Values of adjustable model parameters for the MGLF model are $\varepsilon^*_{12}/k = 558.91$ K, $\delta\varepsilon^*/k = 1010.73$ K, and $\kappa_{11} = -0.3114$. One can notice that ε^*_{11} from the GLF model is underestimated by about 31%. The critical point predicted by the MGLF model shows a slight deviation from the experimental critical point, while the original GLF model shows a large deviation from the expected value.

Figure 6 shows a phase diagram of PS(Mw = 20 400;Mw/Mn ≅ 1.06)/acetone system at 50 bar reported by Zeman *et al.*[24]. The dotted line and the solid line are calculated spinodal curves by the GLF model and the MGLF model, respectively. The prediction of critical point from the MGLF model is slightly above the measured one, however, the GLF model predicts much lower than that of the experimental value. Energy parameter values for the GLF model are $\varepsilon^*_{12}/k = 578.20$ K and $\delta\varepsilon^*/k = 683.49$ K. Values of adjustable model parameters for the MGLF model are $\varepsilon^*_{12}/k = 554.23$ K, $\delta\varepsilon^*/k = 984.18$ K, and $\kappa_{11} = -0.2721$. From the value of κ_{11}, ε^*_{11} is underestimated about 27% by the GLF model. In PS/acetone systems, both ε^*_{12}/k and $\delta\varepsilon^*/k$ decrease with increasing pressure. κ_{11} also decreases with increasing pressure.

CONCLUSIONS

We modified the GLF model by introducing a universal parameter C_0 and a binary parameter κ_{11}. In this study, we fixed $C_0 = 100$ to correct an error in applying Stirling's

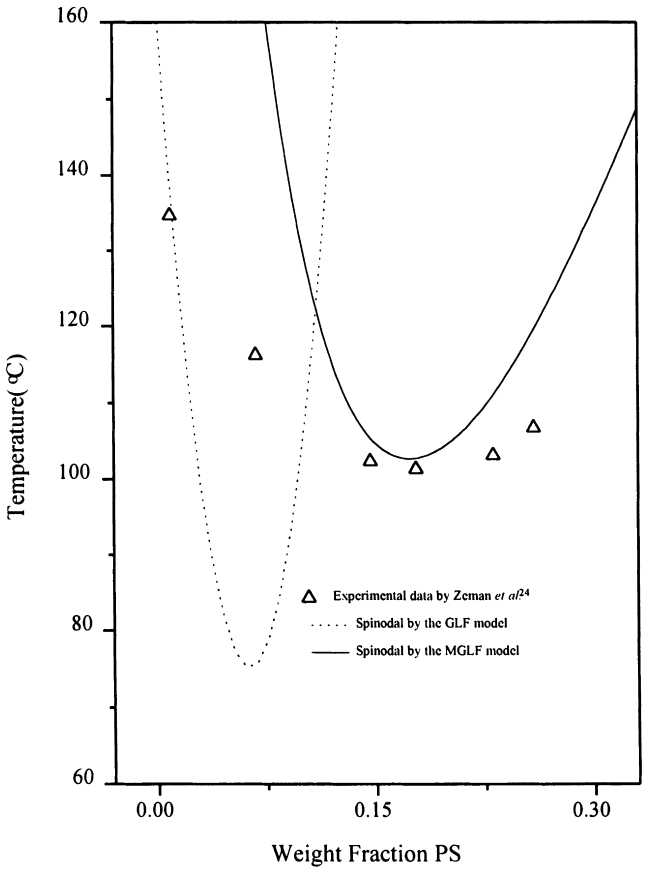

Figure 5 Cloud-point data for PS(Mw = 20 400;Mw/Mn ≅ 1.06)/acetone system at 20 bar. The dotted and the solid line are spinodal curves calculated by the GLF model and the MGLF model, respectively. Energy parameter values for the GLF model are $\varepsilon^*_{12}/k = 589.40$ K and $\delta\varepsilon^*/k = 690.21$ K. Values of adjustable model parameters for the MGLF model are $\varepsilon^*_{12}/k = 558.91$ K, $\delta\varepsilon^*/k = 1010.73$ K, and $\kappa_{11} = -0.3114$. The open up-triangles are experimental data by Zeman *et al.*[24]

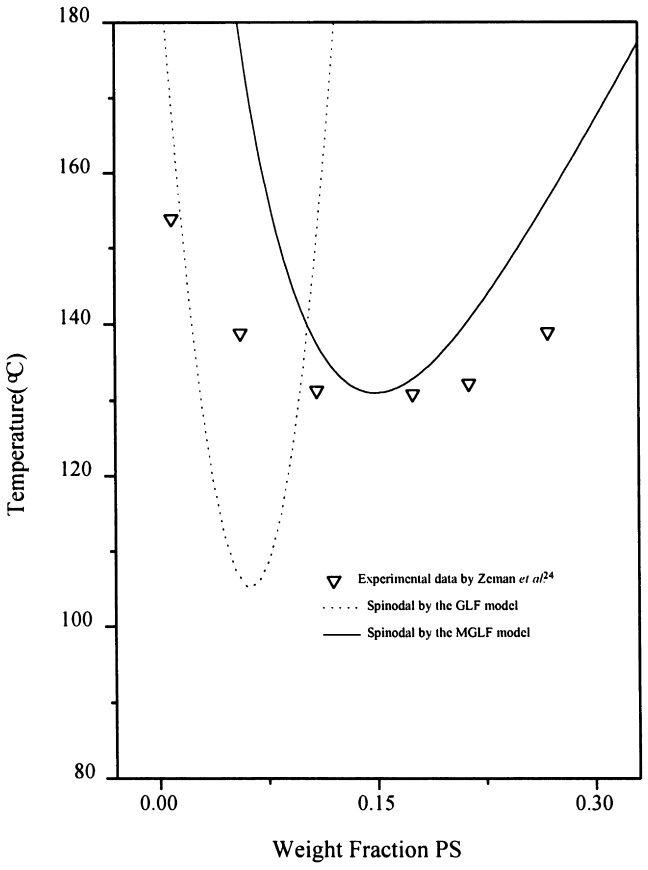

Figure 6 Cloud-point data for PS(Mw = 20 400;Mw/Mn ≅ 1.06)/acetone system at 50 bar. The dotted and the solid line are spinodal curves calculated by the GLF model and the MGLF model, respectively. Energy parameter values for the GLF model are $\varepsilon^*_{12}/k = 578.20$ K and $\delta\varepsilon^*/k = 683.49$ K. Values of adjustable model parameters for the MGLF model are $\varepsilon^*_{12}/k = 554.23$ K, $\delta\varepsilon^*/k = 984.18$ K, and $\kappa_{11} = -0.2721$. The open down-triangles are experimental data by Zeman *et al.*[24]

approximation in the GLF model for polymer solution systems. Our proposed MGLF model predicts and describes remarkably well phase behaviours of polymer solutions at high pressure, while the GLF model shows a large deviation from the experimental data. A new parameter κ_{11} gives a very useful information that can estimate the deviation of ε_{11}^{*} between the value calculated by the GLF model and a real value. The MGLF model is semi-empirical, however it gives very useful practical information with a few adjustable model parameters.

ACKNOWLEDGEMENTS

This research paper was supported by the Korea Science and Engineering Foundation (KOSEF), l997. (No.971-1102-018-2).

REFERENCES

1. Flory, P. J., *J Chem. Phys.*, 1942, **10**, 51.
2. Huggins, M. L., *J. Phys. Chem.*, 1942, **10**, 51.
3. Flory, P. J., *Principles of Polymer Chemistry*, Cornell University Press, Ithaca, NY, 1953.
4. Rodgers, P. A., *J. Appl. Poly. Sci.*, 1993, **48**, 1061.
5. Kleintjens, L. A., Ph.D Thesis, University of Essex, 1979.
6. Kleintjens, L. A. and Koningsveld, R., *Colloid & Polymer Sci.*, 1980, **258**, 711.
7. van Opstal, L. and Koningsveld, R., *Polymer*, 1992, **33**, 3433.
8. Heil, J. F. and Prausnitz, J. M., *AIChE. J.*, 1966, **12**, 678.
9. Brandini, V., *Macromolecules*, 1979, **12**, 883.
10. Panayiotou, C. and Vera, J. H., *Polymer J.*, 1982, **14**, 681.
11. Bae, Y. C., Shim, J. J., Soane, D. S. and Prausnitz, J. M., *J. Appl. Poly. Sci.*, 1993, **47**, 1193.
12. Bae, Y. C., Lambert, S. M., Soane, D. S. and Prausnitz, J. M., *Macromolecules*, 1991, **24**, 4403.
13. Bae, Y. C., *J. Ind. & Eng. Chem.*, 1995, **1**, 18.
14. Sanchez, I. C. and Lacombe, R. H., *J. Phys. Chem.* 1976, **80**, 2352, 2568.
15. Sanchez, I. C. and Lacombe, R. H., *Macromolecules*, 1978, **11**, 1145.
16. Arai, Y. and Saito, S., *J. Chem. Eng. Jap.*, 1972, **5**, 9.
17. Panayiotou, C. and Vera, J. H., *Fluid Phase Equilibria*, 1980, **5**, 55.
18. Sanchez, I. C. and Balazs, A. C., *Macromolecules*, 1989, **22**, 2325.
19. Prigogine, I., *Molecular Theory of Solutions*, North Holland Press, Amsterdam, 1957.
20. Guggenheim, E. A., *Mixtures*, Clarendon Press, Oxford, 1952.
21. Trappaniers, N. J., Schouten, J. A. and Ten Seldam, C. A., *Chem. Phys. Letters*, 1970, **5**, 541.
22. Mulholland, G. W. and Rehr, J. J., *J. Chem. Phys.*, 1974, **60**, 1297.
23. Bonner, D. C., Maloney, D. P. and Prausnitz, J. M., *Ind. Eng. Chem. Process Des. Develop.*, 1974, **13**, 91.
24. Zeman, L., Biros, J., Delmas, G. and Patterson, D., *J. Phys. Chem.*, 1972, **76**, 1206.
25. Liu, D. D. and Prausnitz, J. M., *Ind. Eng. Chem. Process Des. Develop.*, 1980, **19**, 205.
26. Sako, T., Wu, A. H. and Prausnitz, J. M., *J. Appl. Poly. Sci.*, 1989, **38**, 1839.
27. Jang, J. G. and Bae, Y. C., *J. Appl. Polym. Sci.* accepted.
28. Bae, Y. C., Lambert, S. M., Soane, D. S. and Prausnitz, J. M., *Macromolecules*, 1991, **24**, 4403.
29. Saeki, S., Kuwahara, N. and Kaneko, M., *Macromolecules*, 1976, **9**, 101.